Epistemic uncertainty quantification for RANS modeling of the flow over a wavy wall

By C. Gorlé, M. Emory, J. Larsson AND G. Iaccarino

1. Motivation and objectives

While Reynolds-averaged Navier-Stokes (RANS) simulations remain the most affordable technique for simulating complex turbulent flows, the inability of linear eddy viscosity models to correctly predict flow separation and reattachment limits the reliability of the simulation outcome. A methodology to quantify the uncertainty in the simulation outcome related to the form of the turbulence model used, i.e., the epistemic uncertainty, would facilitate using the models for supporting engineering design decisions.

In the present work we address epistemic uncertainty quantification (EUQ) for RANS simulations of the flow over a wavy wall. The goal of the study is to establish a method which can capture the uncertainty in the prediction of the separation region. The methodology used is that proposed in Emory *et al.* (2011) and consists of directly introducing perturbations in the Reynolds stress tensor computed by the model and used in the momentum equations. The perturbations are defined in terms of a decomposition of the Reynolds stress tensor, i.e., its magnitude and the eigenvalue decomposition of the normalized anisotropy tensor. In Gorlé *et al.* (2011), this approach was extended to include EUQ of the mixing model. The perturbation functions used were based on the available LES data set and the method was shown to effectively capture the uncertainty in the mixing of a jet in supersonic cross flow configuration. The goal of the present study, focusing on a more simple flow configuration, is to investigate a more general methodology for defining the perturbation functions. A direct numerical simulation (DNS) database for the configuration from Rossi (2011) will be used for analyzing the turbulence model errors and validating the approach.

The remainder of this research brief is organized as follows. Section 2 introduces the test case considered and summarizes the EUQ methodology used. Section 3 presents the definition of the perturbation functions, mainly focusing on the DNS/RANS comparison for the turbulence kinetic energy. Section 4 presents the results of the resulting EUQ study and the conclusions and future research are presented in Section 5.

2. Methodology

2.1. *Flow setup and DNS database*

The flow setup considered in the present study is identical to the one used in the DNS by Rossi (2011) and is shown in Figure 1. The geometry is defined as a three-dimensional channel, with a flat upper wall and a wavy surface at the lower wall defined by

$$y = A\cos\left(\frac{2\pi x}{\lambda}\right), \tag{2.1}$$

with A the amplitude and λ the wavelength. The wave steepness is defined by $2A/\lambda$ and was equal to 0.1. The DNS database includes results for the flow and for scalar dispersion

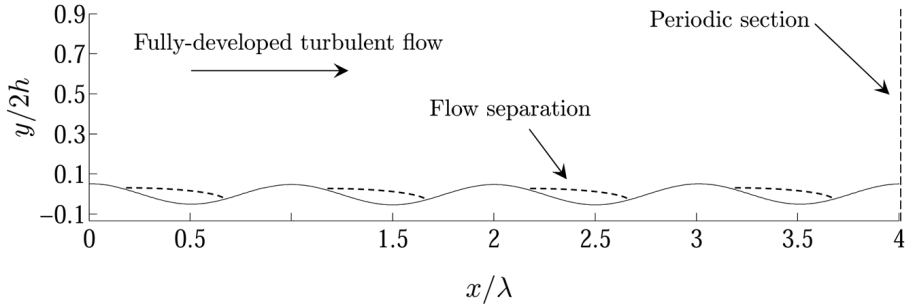

FIGURE 1. Flow configuration (Rossi 2011).

at $Re = 6850$, based on the bulk velocity U_b at the wave crest and the average channel height h. The present study focuses on the solution for the flow field, in particular on the Reynolds stress tensor obtained from the time-averaged DNS solution. The values were also spatially ensemble-averaged in the spanwise direction and over the four wave crests, since the flow is assumed to be fully developed and hence periodic in both directions.

2.2. *RANS simulations*

The RANS simulations were performed on a mesh of 256 x 96 x 128 cells, and the near wall resolution was sufficient ($y^+ \approx 1$) to avoid the use of wall functions. In the streamwise and spanwise direction periodic conditions are applied. Although the flow is two-dimensional, the three-dimensional problem was solved to facilitate including dispersion from a point source in future work. The results presented hereafter were obtained with the SST k-ω model; future work will also consider the realizable k-ϵ model. The uncertainty introduced by these models will be investigated using the methodology from Emory *et al.* (2011), summarized in the following section.

2.3. *EUQ methodology*

In the past, the influence of turbulence models has mainly been investigated by comparing different models, often belonging to the same class of two-equation linear eddy viscosity models. Such traditional sensitivity studies cannot capture the full model form uncertainty, because this uncertainty is largely determined by the model functional form, i.e., the turbulent viscosity hypothesis:

$$\overline{u_i u_j} = \frac{2}{3} k \delta_{ij} - 2\nu_t S_{ij}, \tag{2.2}$$

where $\overline{u_i u_j}$ are the components of the Reynolds stress tensor R_{ij}, k is the turbulent kinetic energy, ν_t is the turbulent viscosity and S_{ij} is the strain rate tensor. To overcome this limitation, a framework for the EUQ of the Reynolds stresses independent of the initial model form was established in Emory *et al.* (2011). The method consists in directly introducing perturbations in the Reynolds stress tensor computed by the model and used in the momentum equations.

The definition of the perturbations is based on reformulating the Reynolds stress tensor in terms of the eigenvalue decomposition of the normalized anisotropy tensor a_{ij}:

$$a_{ij} = \overline{u_i u_j}/2k - \delta_{ij}/3 = v_i \lambda^{(i)} v_j, \tag{2.3}$$

$$\overline{u_i u_j} \approx 2k \left(\frac{\delta_{ij}}{3} + v_i \lambda^{(i)} v_j \right). \tag{2.4}$$

This decomposition involves no modeling assumptions, thereby presenting a general way of introducing epistemic uncertainty in the Reynolds stress tensor:

$$\overline{u_i u_j} + \Delta\overline{u_i u_j} = 2\,(k + \Delta k)\left[\frac{\delta_{ij}}{3} + \Big((v_i + \Delta v_i)(\lambda^{(i)} + \Delta\lambda^{(i)})(v_j + \Delta v_j)\Big)\right], \qquad (2.5)$$

hence specifying the perturbations $\Delta\overline{u_i u_j}$ in terms of a discrepancy in the eigenvalues, $\Delta\lambda^{(i)}$, the eigenvectors, Δv_i, and the turbulence kinetic energy Δk.

In Gorlé *et al.* (2011), this framework was extended to include UQ of turbulent scalar flux models and applied to simulations of a jet in supersonic cross flow configuration. It was shown that the uncertainty in a quantity of interest related to the mixing downstream of the injector could be captured when defining the range of discrepancies considered based on a LES/RANS comparison of the decomposed Reynolds stresses. The remaining challenge is to define the perturbation functions in a more affordable and general way which relies less on the availability of high-fidelity data. This is the focus of the following section.

3. Definition of the perturbation functions

The first consideration is that to avoid an overly conservative estimate of the uncertainty, we should only introduce uncertainty in regions where the model is expected to fail. This leads to the idea of defining a marker which identifies in which regions of the flow perturbations should be introduced. The definition and evaluation of the marker used in the present work is discussed in the first subsection. Subsequently, we need a consistent way of defining the range of perturbations to be considered, which is the focus of the second subsection. The last subsection presents the approach taken in the present study to select the discrete values for the perturbations for which simulations will be performed.

3.1. *Marker definition and evaluation*

The definition of the marker is based on the fact that a scalar turbulent viscosity ν_t can only be unambiguously defined whenever S_{ij} and the deviatoric part of R_{ij} have only a single non-zero component (not counting the symmetric components). Parallel shear flows consistently produce such structure, and, in fact, most validation cases for linear eddy-viscosity models have been for parallel or nearly parallel shear flows: e.g., plane and round jets, mixing layers, channel and boundary layer flows.

It therefore makes sense to define the marker such that it identifies regions in a generic configuration which (locally) resemble parallel shear flows. This can be accomplished by considering the local velocity gradients along the streamlines. Consider a local velocity vector U_i and the unit vector along the streamline $s_i = U_i/\sqrt{U_k U_k}$. The vector

$$g_j = s_i \frac{\partial U_i}{\partial x_j} \qquad (3.1)$$

is then the gradient of the streamline-aligned velocity and the ratio

$$f = \frac{|g_j s_j|}{\sqrt{g_k g_k}} \qquad (3.2)$$

is the cosine of the angle between the direction of the streamline and the gradient of the velocity projected onto the streamline. For perfectly parallel shear flows, with no variation in the streamwise direction (assuming divergence-free velocity), f is exactly

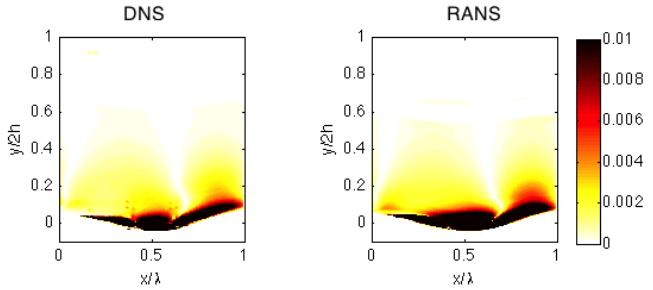

FIGURE 2. Contour levels of the marker from the DNS and baseline RANS SST $k-\omega$ results.

zero. Thus f is a local marker of how far from a parallel shear flow we are. To avoid that the marker becomes undefined in bulk or free-stream flows, or that it includes regions of vanishing turbulence, the actual marker is defined as f scaled by the square of the local turbulence intensity

$$m = f\frac{k}{U_k U_k}. \tag{3.3}$$

While the latter quantity is not Galilean invariant, it does capture the relative magnitude of the Reynolds stress terms compared to the mean convection terms; in other words, approximately the relative importance of the turbulent stresses over the convection.

The marker, as defined by Eq. 3.3, is a function of the mean flow properties only and was computed using the averaged DNS flow field and the flow field obtained from the baseline RANS simulation with the SST $k-\omega$ model. The result is shown in Figure 2 and indicates that the marker values look similar when using the correct (DNS) or the modeled (RANS) flow field. In both cases the marker values are higher in the separated flow region.

To quantify the effectiveness of the marker at highlighting the regions in the flow where the turbulence model fails, a performance metric was defined. The metric is based on a comparison of the divergence of the Reynolds stress tensor, $\partial_j R_{ij}$, from the DNS and the RANS, since this is the term occurring in the momentum equations. When this difference is small, the RANS model will produce an accurate prediction of the mean flow. The marked regions should therefore correspond to regions where the difference in $\partial_j R_{ij}$ from the DNS and the RANS is large. A contour plot of the values and the difference between RANS and DNS for the two components of the divergence are shown in Figure 3. From a comparison with Figure 2, it can be observed that higher values of the marker correspond to larger differences in $\partial_j R_{ij}$.

The performance of the marker can subsequently be quantified by constructing Table 1. The points were flagged as 'Marker ON' when the value of the marker was higher than 10^{-3} and as 'RANS $\neq$ DNS' when the difference between the RANS and DNS Reynolds stress divergence was higher than 1% of U_b^2 in one or both components.

The table shows that, given the chosen threshold, the marker correctly classifies 69% of the points. It gives a conservative classification in 18% of the points, where the marker will introduce perturbations while the model is working correctly. More importantly, however, the marker does not identify model failure in another 18% of the points. To illustrate where these points are located, Figure 4 indicates in which locations the marker is ON and in which regions the difference between RANS and DNS is larger than 1%

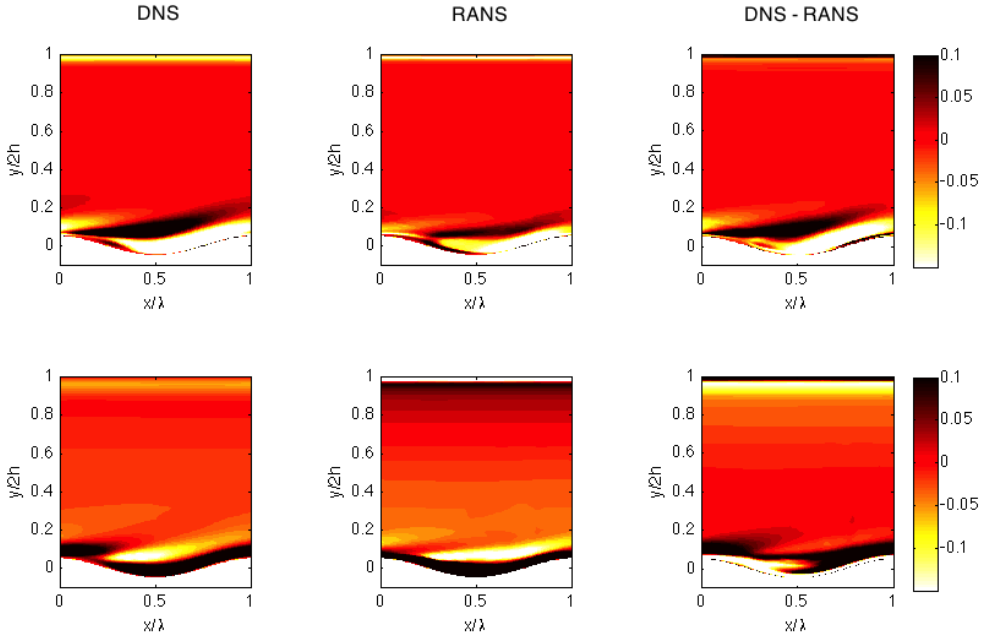

FIGURE 3. DNS and RANS values of the divergence of the Reynolds stress tensor, including the difference. Top row: streamwise component, lower row: wall-normal component.

TABLE 1. Marker Performance: 'Marker ON' for $m > 10^{-3}$, 'RANS $\neq$ DNS' when the difference between $\partial_j R_{ij} > 0.01 U_b^2$ in one or both components.

	RANS $\neq$ DNS	RANS = DNS
Marker ON	18%	18%
Marker OFF	13%	51%

of U_b^2. It is observed that the majority of the points where the marker is OFF and the difference in the divergence of the Reynolds stress tensor is larger than 1% of U_{inf}^2 is near the upper wall. This region accounts for 15% of the total number of points and it is the prediction of the wall-normal component of $\partial_j R_{ij}$ that fails. The region does correspond to parallel shear flow, and the prediction of the wall-normal component of $\partial_j R_{ij}$ will not influence the flow solution, hence it is desirable that the marker is not active.

3.2. *Range of perturbations*

As introduced in Section 2.3, the perturbations $\Delta\overline{u_i u_j}$ are specified in terms of a discrepancy in the eigenvalues, $\Delta\lambda^{(i)}$, the eigenvectors, Δv_i, and the turbulence kinetic energy Δk.

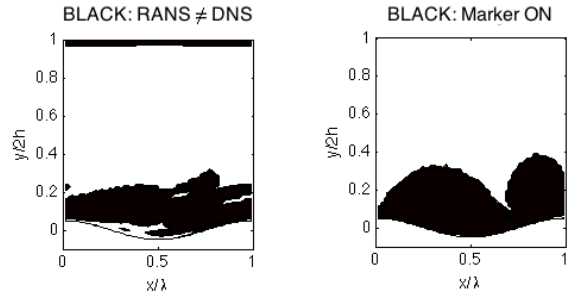

FIGURE 4. Spatial distribution of DNS/RANS discrepancy (right) and marker based on the RANS solution (left). Marked regions have $\Delta\left(\partial_j R_{ij}\right) > 0.01 U_b^2$ or $m > 10^{-3}$
.

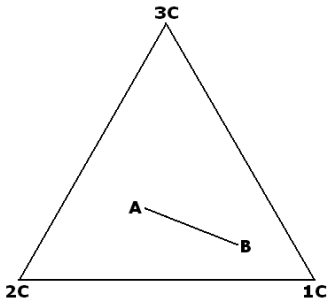

FIGURE 5. Barycentric map.

3.2.1. *Perturbation of eigenvalues*

The perturbation of the eigenvalues λ_i of the Reynolds stress anisotropy tensor is based on modifying their location within the barycentric map (Banerjee *et al.* 2007) shown in Figure 5. The map contains all the realizable states of the Reynolds stress tensor and its corners represent different limiting states of turbulence anisotropy, referred to by their corresponding number of components, e.g., isotropic turbulence corresponds to the three-component (3C) corner. The unique location within the map is determined by a linear combination of λ_i. The procedure to define the perturbations in the eigenvalues $\Delta\lambda^{(i)}$ is to first determine the map location of the Reynolds stress computed by the $k-\omega$ SST turbulence model (A) and subsequently inject uncertainty by moving it to a new location (B). Once the new location has been determined, an updated set of eigenvalues corresponding to $\left(\lambda_i + \Delta\lambda^{(i)}\right)$ is evaluated and used to reconstruct a_{ij} and the Reynolds stress tensor (Emory *et al.* 2011). This procedure imposes clear bounds on the possible perturbations, since it is restricted to representing realizable states of turbulence located inside the triangular map.

3.2.2. *Perturbation of eigenvectors*

Perturbations of the eigenvectors, Δv_i, can be defined in terms of a rotation of the principal axes of the anisotropy tensor, hence bounding the uncertain variables, i.e., the Euler angles, between 0 and 2π. In the present configuration, where the flow field is two-dimensional, only one rotation angle can be defined in order to retain only one non-zero off-diagonal stress component.

3.2.3. *Perturbation of turbulence kinetic energy*

To define a realistic range of perturbations for the turbulence kinetic energy, the discrepancies in k between the RANS and DNS simulations were analyzed. Three different sets of simulations were performed. First, both the RANS flow and turbulence equations were solved. Second, the effect of the coupling to the mean flow was eliminated by freezing the flow to the averaged DNS flow field, solving the transport equations for the turbulence quantities, k and ω only. Third, the turbulence kinetic energy production term was also frozen to the exact production term calculated from the DNS as $P_k = -\overline{u_i u_j}\frac{\partial U_i}{\partial x_j}$. The difference between the last two sets of simulations is that when only freezing the DNS flow field, P_k is still determined from the inexact Reynolds stresses as computed using the turbulent viscosity hypothesis, whereas in the second case the exact Reynolds stresses are used.

Figure 6 presents the comparison for the turbulence kinetic energy from the DNS and from the three different simulations with the SST $k-\omega$ model. The result shows an underprediction of the order of 100% when solving the coupled momentum and turbulence transport equations. When removing the coupling to the mean flow, the turbulence kinetic energy decreases further, increasing the level of discrepancy. However, when using the correct production term for k, a much higher accuracy in the prediction is obtained.

Based on this observation, it can be concluded that the incorrect value for P_k is a major reason for errors in the prediction of the turbulence kinetic energy. Hence, it was decided to perturb k indirectly by perturbing the production term. This perturbation can leverage the perturbations already introduced in the eigenvalues and the eigenvectors, by using the reconstructed perturbed Reynolds stress tensor in the exact formulation for the production term.

3.3. *Defining systematic perturbations*

By defining the perturbations for the different quantities as described above, the question of defining bounds has been addressed. Subsequently, we need a systematic methodology to select the discrete values of the perturbations within these bounds for which simulations will be performed. In the present study, only spatially uniform perturbation functions are considered; introducing spatial variations will be the focus of future work.

Systematic perturbations of the eigenvalues have been defined by perturbing the eigenvalues towards one of the three limiting states of turbulence, i.e., making the Reynolds stress tensor more isotropic (towards C3), more two-component (towards C2) or more one-component (towards C1). The procedure takes the original eigenvalues for every point in the domain and moves them with a predefined fraction towards the corners. For the eigenvectors, a systematic perturbation could consider a number of values for the Euler angle of interest for this two-dimensional flow field. The combination of the different perturbations would, however, result in a relatively large number of simulations.

In order to select an initial smaller subset of simulations, and considering the importance of the production term for the turbulence kinetic energy demonstrated in the previous section, the initial values for the perturbations of the eigenvalues and eigenvectors were selected as those which produce the maximum and minimum production term integrated over the marked region. The integrated production was therefore computed for the range of possible movements within the barycentric map as defined above for different rotation angles. Figure 7 presents the resulting contour plot of the integrated value of P_k for three rotation angles: 0°, 15° and 30°. The location of the values in the barycentric map corresponds to the fraction of movement of the eigenvalues towards the

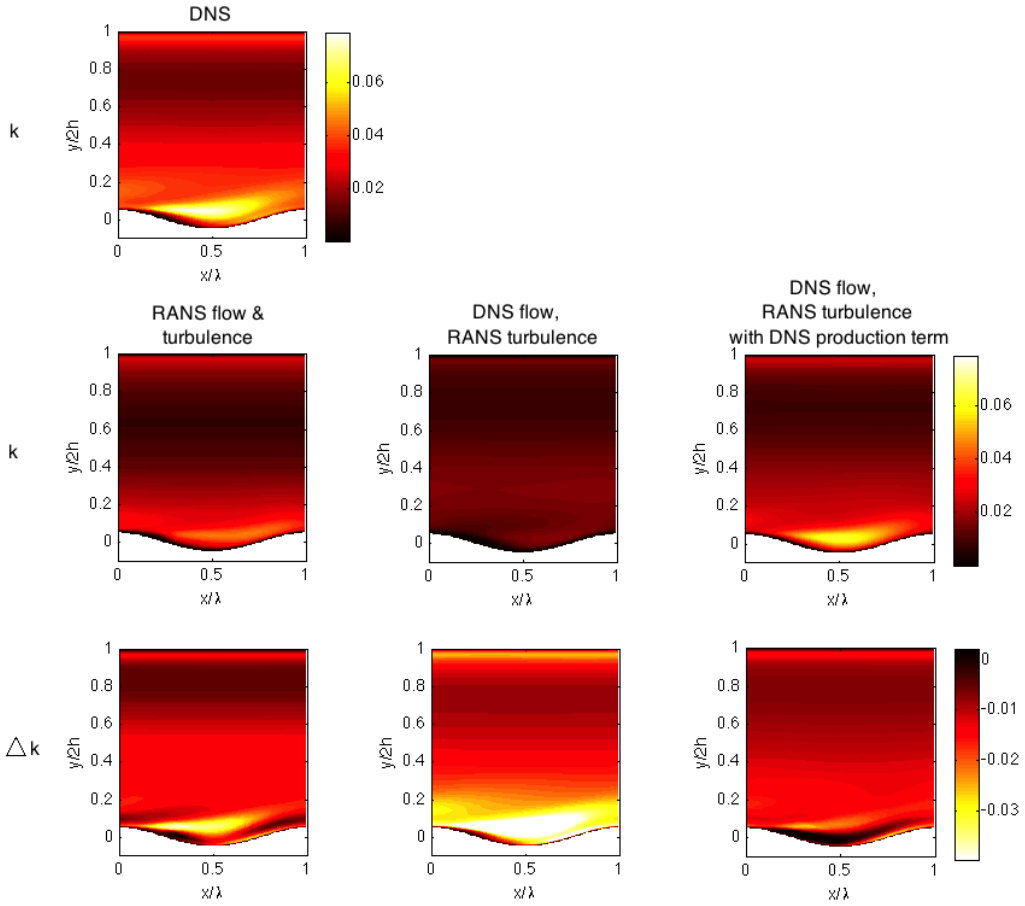

FIGURE 6. Comparison of k from DNS and SST $k-\omega$ models, solving the coupled momentum and turbulence transport equations, solving the turbulence transport equations with the DNS mean flow field and solving the turbulence transport equations with the DNS mean flow field and DNS production term for k.

borders of the map, with the origin the centerpoint of the triangle. The plots show that the extreme values are found when only modifying the eigenvalues, with the maximum occurring when moving towards the one-component corner and the minimum when moving towards the three-component corner. Since perturbations all the way to the corner of the map are expected to be too conservative, the magnitude was restricted to movements that go halfway to the corners.

To visualize the resulting perturbations of P_k, Figure 8 shows the contours of the turbulent production term from the DNS, the unperturbed RANS model and the RANS model with the perturbations that produce $P_{k,max}$ and $P_{k,min}$. Table 2 includes the integrated values. The contours demonstrate that with the present methodology a realistic perturbation can be obtained. In addition, the integrated values actually encompass the DNS value.

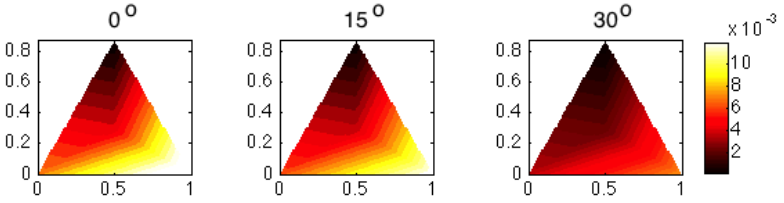

FIGURE 7. Contour plot of the turbulent production integrated over the marked region for three rotation angles: 0°, 15° and 30°. The location of the values in the barycentric map corresponds to the fraction of movement of the eigenvalues towards the borders of the map, with the origin the centerpoint of the triangle.

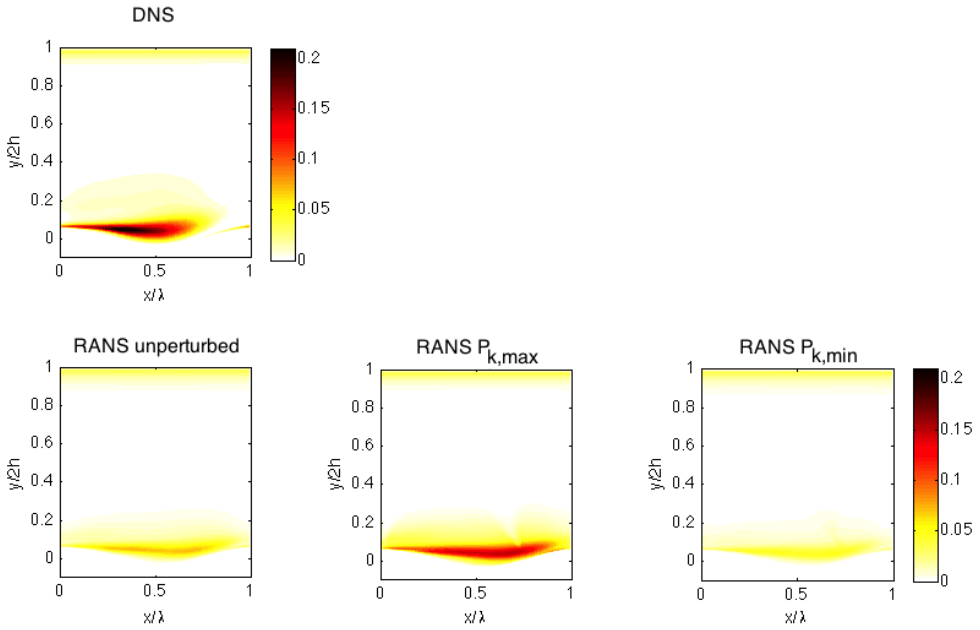

FIGURE 8. Contours of the turbulent production from the DNS, the unperturbed RANS $k-\omega$ model and the RANS $k-\omega$ model with the perturbations that produce $P_{k,max}$ and $P_{k,min}$.

TABLE 2. Turbulent production term integrated over the marked region from the DNS, the unperturbed RANS $k-\omega$ model and the RANS $k-\omega$ model with the perturbations that produce $P_{k,max}$ and $P_{k,min}$.

	DNS	RANS unperturbed	$P_{k,min}$	$P_{k,max}$
P_k	0.0083	0.0045	0.0094	0.0024

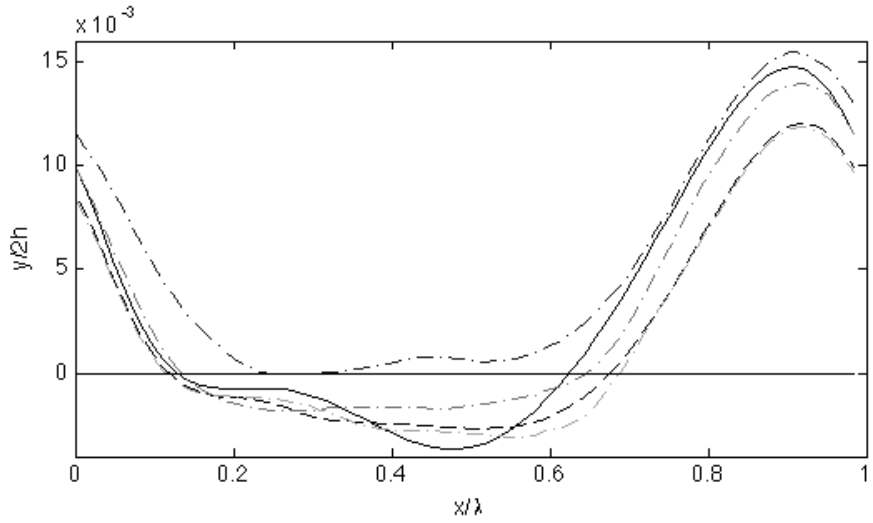

FIGURE 9. Streamwise component of the wall shear stress for the DNS (——), the baseline RANS SST $k-\omega$ (– –) and three perturbed runs: perturbation towards C1 for $P_{k,max}$ (– ·), perturbation towards C3 for $P_{k,min}$ (– ··) and perturbation towards C2 (– ·).

4. Results

The results are presented in terms of the streamwise component of the wall shear stress along the wavy wall to clearly indicate the separation and reattachment points. Figure 9 includes the values from the DNS, the baseline RANS SST $k-\omega$ and the perturbed runs corresponding to $P_{k,min}$ and $P_{k,max}$ as prescribed in the previous section. An additional run with a perturbation towards the two-component corner of the barycentric map is included as well. The result shows the promising capabilities of the approach in capturing the uncertainty in the reattachment location. In addition, the uncertainty in the wall shear stress is captured at almost all streamwise locations along the wave crest.

5. Conclusions and Future Work

The goal of the present study was to establish a method which can capture the uncertainty in the prediction of the separation region for the flow over a wavy wall.

The methodology used is based on the framework presented in Emory *et al.* (2011) and consists in directly introducing perturbations in the Reynolds stress tensor computed by the model and used in the momentum equations. The perturbations are defined in terms of a decomposition of the Reynolds stress tensor, i.e., its magnitude and the eigenvalue decomposition of the normalized anisotropy tensor. The definition of the perturbation functions is based on two basic concepts:

(*a*) A marker, which identifies regions that deviate from parallel shear flow as regions where perturbations should be introduced.

(*b*) Systematic perturbations in the marked region by (1) moving the eigenvalue of the anisotropy tensor towards the one-, two- or three-component corners; (2) rotating the eigenvectors with the Euler angle that preserves the two-dimensionality of the flow; and (3) using the turbulence production term computed with the modified anisotropy tensor to perturb the turbulence kinetic energy.

Simulations were performed for the perturbations which result in the maximum and

minimum production term integrated over the marked region. These were found when changing the eigenvalues to the one- and three-component corners of the map, respectively. It was shown that these two simulations capture the uncertainty in the size of the separated region and give a very realistic representation of the streamwise wall shear stress. An additional simulation with perturbations towards the two-component corner shows an improved agreement with the DNS data on the wave crest, indicating that a model capable of predicting two-component turbulence in this region could provide better results.

Future work will focus on a further analysis of these results and extend the methodology to incorporate uncertainty quantification of dispersion over the wavy wall. In addition, the introduction of spatially varying perturbations will be considered. This should, for example, allow us to account for different discrepancies on the downhill and uphill part of the wave trough.

Acknowledgments

This material is based upon work supported by the Department of Energy [National Nuclear Security Administration] under award number NA28614.

REFERENCES

Banerjee, S., Krahl, R., Durst, F. & Zenger, C. 2007 Presentation of anisotropy properties of turbulence, invariants versus eigenvalue approaches. *J. Turb.* **8**, 1–27.

Emory, M., Pecnik, R. & Iaccarino, G. 2011 Modeling structural uncertainties in Reynolds-averaged computations of shock/boundary layer interactions. *AIAA paper* **2011-0479**.

Gorlé, C., Emory, M. & Iaccarino, G. 2011 Epistemic uncertainty quantification of RANS modeling for an underexpanded jet in a supersonic cross flow. *Ann. Res. Briefs 2011, Center for Turbulence Research, Stanford, CA* pp. 147–159.

Rossi, R. 2011 A numerical study of algebraic flux models for heat and mass transport simulation in complex flows. *Int. J. Heat and Mass Transfer* **53**, 4511–4524.